Immunoglobulin D enhances immune surveillance by activating antimicrobial, pro-inflammatory and B cell-stimulating programs in basophils

Kang Chen, Weifeng Xu, Melanie Wilson, Bing He, Norman W. Miller, Eva Bengten, Eva-Stina Edholm, Paul A. Santini, Poonam Rath, April Chiu, Marco Cattalini, Jiri Litzman, James Bussel, Bihui Huang, Antonella Meini, Kristian Riesbeck, Charlotte Cunningham-Rundles, Alessandro Plebani, Andrea Cerutti

SUPPLEMENTARY FIGURE LEGENDS S1 – S11

SUPPLEMENTARY TABLES S1 – S2

SUPPLEMENTARY FIGURES S1– S11

SUPPLEMENTARY FIGURE LEGENDS

Figure S1. Detection of IgD^+IgM^- plasmablasts in follicular and extrafollicular areas of the upper respiratory mucosa and peripheral blood. (**a**, **b**) Immunofluorescence analysis of tonsil tissue stained for IgD (green) and IgM (red). DAPI (blue) counterstains nuclei. Dashed and dotted lines demarcate follicular and subepithelial areas, respectively. Arrowheads point to follicular and extrafollicular IgD^+IgM^- plasmablasts. In b, box shown in upper panel includes a mucosal area that was further magnified in bottom panels. Note that many of the IgD^-IgM^+ cells visualized in the germinal center correspond to follicular dendritic cells capturing IgM-containing immunocomplexes. Original magnification, ×10. (**c**) Tonsil tissue stained for IgD (green), CD19 (red) and IgM (blue). DAPI (blue) counterstains nuclei. Arrowheads in bottom panels point to magnified $IgD^+IgM^-CD19^+$ plasmablasts from boxed area in upper panel. Original magnification, ×10 (upper panels) and ×40 (bottom panels). (**d**) Flow cytometric analysis of CD5, CD10, CD19, CD20, CD21, CD22, CD23, CD24, CD27, CD38, CD39, CD40, CD77, CD138, BAFF-R, TACI, BCMA, Pax5, Blimp-1, κ, λ, Ki-67, MHC-I and MHC-II on IgD^+IgM^+ (gate G1, blue histograms) and IgD^+IgM^- (gate G2, red histograms) B cells from tonsils. These B cells were also stained with hematoxylin and eosin after FACSorting. Original maginification, ×40. (**e**) CD5, CD10, CD21, CD23, CD27 and CD38 on IgD^+IgM^+ (blue histograms) and IgD^+IgM^- (red histogram) B cells from peripheral blood. Panels a-e show 1 of 5 experiments yielding similar results.

Figure S2. Class switching from IgM to IgD occurs in response to CD40L, BAFF or APRIL combined with IL-2 plus IL-21. (**a**) Flow cytometric analysis of CD19, IgM and IgD on peripheral blood IgD^+IgM^+ B cells used for class switch experiments. Gray histogram shows an isotype-matched control. (**b**) IgD and IgM expression on peripheral blood IgD^+IgM^+ B cells exposed to CD40L, BAFF or APRIL and a combination of IL-2 plus IL-21 for 7 days. (**c**) ELISA of IgD secreted by peripheral blood IgD^+IgM^+ B

cells stimulated as in b. (**d**) IgD and IgM expression on peripheral blood IgD^+IgM^+ B cells exposed to individual or combined cytokines (IL-2, IL-4, IL-10, IL-13, IL-15 or IL-21) in the presence or absence of CD40L, BAFF or APRIL for 7 days. Panels a, b and c show 1 of 3 experiments yielding similar results, whereas panel c summarizes 3 experiments (bars indicate s.e.m.).

Figure S3. Class switching from IgM to IgD is absolutely dependent on AID, but only partially dependent on CD40. (**a**) Percentage of circulating IgD^+IgM^- plasmablasts in patients with *TNFSF5* (HIGM1, 3 cases) or *AICDA* (HIGM2, 3 cases) gene defects. (**b**) Immunofluorescence analysis of extrafollicular plasmablasts from the mucosa of a healthy individual or patients with *TNFRSF5* (HIGM3) or *AICDA* (HIGM2) gene defects stained for IgD (green) and IgM (red). DAPI (blue) counterstains nuclei. Note double-positive IgD^+IgM^+ plasmablasts in both HIGM2 and HIGM3 tissue sections as well as residual class-switched IgD^+IgM^- plasmablasts in the HIGM3 tissue section. Original magnification, ×40. (**c**) Tonsil tissue from a HIGM2 patient stained for IgD (green) and IgM (red). DAPI (blue) counterstains nuclei. Dashed lines demarcate primary follicles. Follicular double-positive IgD^+IgM^+ plasmablasts from upper panel are shown magnified in bottom panels. Original magnification, ×10 (upper panels) and ×40 (bottom panels). (**d**) Flow cytometric analysis of IgM and IgD on gated $CD19^+$ B cells from a healthy subject and two HIGM2 patients incubated with medium alone (control) or BAFF plus IL-2 plus IL-21 for 5 days. Due to the limited amount of HIGM2 blood specimens, the experiment was performed with peripheral blood mononuclear cells and involved surface Ig triggering by an anti-IgM antibody to obtain maximal activation and expansion of the B cells present in the culture. Panels a-d show 1 of 3 experiments yielding similar results.

Figure S4. Polyclonal and monoclonal anti-IgD antibodies specifically detect IgD on the surface of basophils. (**a**) Percentage of IgD-armed basophils in three healthy donors as determined by stainings performed with either a goat $F(ab')_2$ pAb to IgD or a mouse IA6-2 mAb to IgD. Neutrophils, eosinophils

and B cells are shown for comparison. (**b**) Comparable IgD profiles on basophils, neutrophils, eosinophils and B cells stained with either a goat $F(ab')_2$ pAb to IgD or a mouse IA6-2 mAb to IgD. Panels a-d show 1 of 3 experiments yielding similar results.

Figure S5. IgD binds to both basophils and mast cells *in vivo*. (**a**) Flow cytometric analysis of IgD on viable (7-AAD$^-$) basophils, neutrophils, eosinophils, monocytes and myeloid dendritic cells (mDCs) from the peripheral blood of healthy individuals. A $F(ab')_2$ pAb was used to detect IgD. Mean fluorescence intensity (MFI) was the ratio between the fluorescence intensity of IgD-stained cells and the fluorescence intensity of unstained cells. The dashed line indicates average MFI for IgD on basophils. (**b**) Flow cytometric analysis of IgD, IgE, CD117 and FcεRI on viable (7-AAD$^-$) lung mast cells. A $F(ab')_2$ pAb was used to detect IgD. Controls (gray histograms) include cells stained with appropriate isotype-matched antibodies with irrelevant binding activity (CD117 and FcεRI) or unstained cells (IgE or IgD). (**c**) IgD, CD117 and FcεRI on viable circulating mast cells from two patients with mastocytoma. IgD was detected with a $F(ab')_2$ pAb and then analyzed on gated CD117$^+$FcεRI$^+$ cells. FSC and SSC are forward and side scatters, respectively. (**d**) Immunofluorescence of tonsil from a healthy subject stained for IgD (green), tryptase, CD117 or CD123 (red), and FcεRI (blue). DAPI counterstains nuclei. Dashed line demarcates follicles. Arrowheads point to IgD^{low}CD117$^+$tryptase$^+$CD123$^-$ mast cells (MC), IgD^{high}CD117$^-$tryptase$^+$CD123$^+$ basophils (Basø), and IgD^{high}CD117$^-$tryptase$^-$CD123$^-$ plasmablasts (B). Dashed line demarcates follicle. Original magnification, ×10 (uppermost panels) and ×40 (bottom panels). Panels a-d show 1 of 3 experiments yielding similar results.

Figure S6. IgD-detecting $F(ab')_2$ antibody does not cross-react with IgG. (**a**) IgD binding profile of HMC-1 mastocytoid, KU812 pre-basophilic and U937 monocytoid cell lines incubated with a goat $F(ab')_2$ pAb to IgD in the absence of exogenous monoclonal IgD. (**b**) IgD and IgG binding profiles of HMC-1, KU812 and U937 cell lines incubated with a goat $F(ab')_2$ pAb to IgD or a goat $F(ab')_2$ pAb to

IgG upon incubation with exogenously added polyclonal IgG. (**c**) Percentage of IgD-binding KU812 cells upon incubation with IL-3 for 2 days and subsequent exposure to monoclonal IgD. Stainings were performed with either a goat $F(ab')_2$ pAb to IgD or a mouse IA6-2 mAb to IgD or a mouse IgD26 mAb to IgD. (**d**) Percentage of IgD-binding HMC-1 cells incubated with either polyclonal IgD from normal plasma or monoclonal IgD from a multiple myeloma patient and then stained with a goat $F(ab')_2$ pAb to IgD. Panels a-d show 1 of 3 experiments yielding similar results.

Figure S7. Basophilic and mastocytoid cell lines up-regulate binding of IgD upon undergoing maturation in response to IL-3 or IL-4. (**a**) Flow cytometric analysis of monoclonal IgD binding to basophilic KU812 cells cultured in the presence or absence of IL-3 for 4 days. KU812 cells were stained for IgD with a $F(ab')_2$ pAb and for surface CD117, CD124 (IL-4R) and FcεRI with appropriate mAbs. Unlike non-malignant basophils, KU812 cells expressed surface CD117. Numbers denote percentage of positive cells. Dead cells were excluded using 7-AAD. (**b**) Binding of monoclonal IgD to LAD2 mast cells cultured in the presence or absence of IL-4 for 4 days. LAD2 cells were also stained for surface CD123. A $F(ab')_2$ pAb was used to detect IgD. Dead cells were excluded using 7-AAD. Panels a and b show 1 of 3 experiments yielding similar results.

Figure S8. IgD^+IgM^- plasmablasts and IgD-armed granulocytes in channel catfish. (**a**) Flow cytometric analysis of IgM and IgD on circulating lymphocytes from a representative fish. IgD^+IgM^- plasmablasts (red gate) as well as IgD^+IgM^+ and IgD^-IgM^+ lymphocytes (blue gate) were studied for morphology by Giemsa and for expression of transcripts encoding membrane (m) and secreted (s) IgM and IgD by RT-PCR. FSC and SSC, forward and side scatter. **(b**) Flow cytometric analysis of IgM (blue histogram) and IgD (red histogram) on circulating mononuclear cells from a different fish. Gates G1 and G2 correspond to canonical lymphocytic and granulocytic cells, respectively. The black histogram is an isotype-matched control. **(c**) Granular IgD^+IgM^- cells were sorted from fish leukocytes shown in b to study their

morphology as well as expression of transcripts encoding IgM and IgD. Elongation factor-1a (EF-1α) transcript is a loading control. Panels a-c show 1 of 5 experiments yielding similar results.

Figure S9. IgD or IgE cross-linking induces distinct patterns of surface CD63, BAFF, APRIL and CD40L expression on basophils. Flow cytometric analysis of CD63, BAFF, APRIL and CD40L on basophils exposed to microbeads alone (control), microbead-bound monoclonal anti-IgD, or microbead-bound monoclonal anti-IgE in the presence or absence of IL-3 for 30 min, 16 h or 48 h. Numbers denote percentage of cells in each quadrant. Dead cells were excluded using 7-AAD staining. Data depict 1 of 3 experiments yielding similar results.

Figure S10. Dysregulation of IgD class-switched plasmablasts and IgD-armed basophils in patients with autoinflammatory syndrome and periodic fever. (**a, b**) Flow cytometric analysis of circulating $IgD^{+}IgM^{-}$ plasmablasts and IgD-armed $CD123^{+}HLA\text{-}DR^{-}$ basophils in healthy individuals and patients with MWS (1 case), HIDS (4 cases), PFAPA (3 cases), and TRAPS (5 cases). The dashed line indicates the average percentage of plasmablasts and basophils within B cells and mononuclear cells, respectively, in healthy individuals. IgD was stained with a $F(ab')_2$ pAb. Dead cells were excluded using 7-AAD. (**c**) Immunofluorescence analysis of tonsillar tissue from a patient with PFAPA syndrome stained for APRIL or LL-37 (green), CD117 or CD123 (red), and FcεRI (blue). DAPI counterstains nuclei (note lobated nuclei of basophils). Arrowheads point to activated $APRIL^{+}CD117^{-}FcεRI^{+}$ or $LL\text{-}37^{+}CD123^{+}FcεRI^{+}$ basophils (Basø) from extrafollicular areas. Original magnification, ×40. Panels a-c show 1 of 3 experiments yielding similar results.

Figure S11. Model of IgD regulation and function. B cells from the upper respiratory mucosa undergo CSR from C_μ to C_δ through local TD and TI pathways involving CD40L, BAFF or APRIL together with a unique cocktail of cytokines, including IL-2 and IL-21 or IL-15 and IL-21. CSR requires AID and generates mucosal and circulating plasmablasts that secrete IgD antibodies reactive against respiratory

bacteria. Mucosal IgD might enhance local immunity after translocating across epithelial cells, whereas circulating IgD binds to basophils via a calcium-mobilizing receptor. In addition to delivering rapid innate responses and alerting the immune system as to the presence of invading bacteria, basophils exposed to IgD-reactive antigens migrate to systemic and mucosal lymphoid organs, perhaps in response to chemotactic factors released by IgD-stimulated mast cells. Tissue-based basophils enhance immune protection by releasing antimicrobial, opsonizing, B cell-stimulating, chemotactic and pro-inflammatory mediators such as cathelicidin, IL-1, IL-4, IL-8, IL-13, CD40L, BAFF, APRIL, TNF and CXCL10, but not histamine. Finally, IgD-armed basophils may regulate B cell homeostasis through tonic release of the obligatory B cell survival factor BAFF in response to IgD-reactive foreign or autologous antigens.

SUPPLEMENTARY TABLES

Table S1 Antibodies used in flow cytometry and immunofluorescence

a. Flow cytometry

Antigen | [Epitope]	Label	Isotype	Clone (if monoclonal)	Manufacturer	Note
AID	-	Mouse IgG1	C12.38	German Cancer Research Center	
APRIL [AT125]	-	Rabbit IgG	-	Alexis	Specific to membrane-expressed APRIL, not soluble APRIL or soluble APRIL that binds to cell membrane.
BAFF (CD257)	PE	Mouse IgG1	1D6	eBioscience	
	Biotin	Mouse IgG1	1D6	eBioscience	
BAFF-R (CD268)	PE	Mouse IgG1	11C1	BD Biosciences	
BCMA [N-16]	-	Goat IgG	-	Santa Cruz	
Blimp-1	-	Mouse IgG1	3H2-E8	Novus Biologicals	
CD3	FITC	Mouse IgG1	UCHT1	Ancell	
	Biotin	Mouse IgG1	UCHT1	BD Biosciences	
CD4	FITC	Mouse IgG2b	M-T441	Ancell	
	Biotin	Mouse IgG1	SK3	BD Biosciences	
CD5	PE	Mouse IgG1	UCHT2	BD Biosciences	
CD8	PE	Mouse IgG2a	UCHT4	Sigma	
CD10	PE	Mouse IgG1	ALB1	Immunotech	
CD11c	PE	Mouse IgG1	B-ly6	BD Biosciences	
CD14	PE	Mouse IgG2a	UCHM-1	Sigma	
	Biotin	Mouse IgG2a	UCHM-1	Southern Biotech	
CD15	FITC	Mouse IgM	28	Southern Biotech	
CD16	Biotin	Mouse IgG1	3G8	BD Biosciences	
CD19	FITC	Mouse IgG1	SJ25-C1	Southern Biotech	
	PE	Mouse IgG1	4G7	BD Biosciences	
	APC	Mouse IgG1	H1B19	BD Biosciences	
	Pacific Blue	Mouse IgG1	H1B19	BioLegend	
	Biotin	Mouse IgG1	H1B19	BD Biosciences	

CD20	FITC	Mouse IgG1	L27	BD Biosciences	
CD21	PE	Mouse IgG1	B-ly4	BD Biosciences	
CD22	-	Mouse IgG1	FPC1	Novocastra	
CD23	FITC	Mouse IgG1	9P25	Immunotech	
CD24	PE	Mouse IgG2a	ML5	BD Biosciences	
CD27	FITC	Mouse IgG1	M-T271	BD Biosciences	
	PE	Mouse IgG1	M-T271	Ancell	
	APC	Mouse IgG1	O323	eBioscience	
CD38	PE	Mouse IgG1	HIT2	BD Biosciences	
CD39	-	Mouse IgG1	BU61	Binding Site	
CD40	FITC	Mouse IgG1	BE-1	Ancell	
CD56	FITC	Mouse IgG2b	NCAM16.2	BD Biosciences	
CD63	FITC	Mouse IgG1	AHN16.1/46-4-5	Ancell	
	Biotin	Mouse IgG1	AHN16.1/46-4-5	Ancell	
CD80	FITC	Mouse IgM	BB1	BD Biosciences	
CD83	FITC	Mouse IgG1	HB15e	Ancell	
CD86	PE	Mouse IgG2b	IT2.2	BD Biosciences	
CD95 (Fas)	PE	Mouse IgG1	DX2	BD Biosciences	
CD117	PE	Mouse IgG1	104D2	BD Biosciences	
CD123	PE	Mouse IgG2a	7G3	BD Biosciences	
	APC	Mouse IgG1	6H6	eBioscience	
CD124	Biotin	Mouse IgG1	hIL4R-M57	BD Biosciences	
CD138	PE	Mouse IgG1	Mi15	BD Biosciences	
CD154 (CD40L)	PE	Mouse IgG1	24-31	Ancell	
FcεRIα	Biotin	Mouse IgG2b	AER-37	eBioscience	
HLA-DR	FITC	Mouse IgG2a	L243	BD Biosciences	
	PE	Mouse IgG2a	L243	BD Biosciences	
IgA	FITC	Goat IgG	-	Sigma Aldrich	
	PE	Goat IgG $F(ab')_2$	-	Southern Biotech	
	Biotin	Goat IgG $F(ab')_2$	-	Southern Biotech	
IgD	FITC	Goat IgG $F(ab')_2$	-	Southern Biotech	Used to detect IgD levels on different primary cells and cell lines. Does not cross-react with IgG.
	FITC	Mouse IgG2a	IA6-2	BD Biosciences	Tested to yield similar IgD profile as the
	Biotin	Mouse IgG2a	IADB6	Southern Biotech	

	PE	Mouse IgG1	IgD26	Santa Cruz	above FITC-conjugated goat F(ab')2 anti-IgD antibody.
IgE	FITC	Goat IgG	-	CAPPEL	
	Biotin	Goat IgG $F(ab')_2$	-	Southern Biotech	
	Biotin	Mouse IgG2a	G7-26	BD Pharmingen	
IgM	FITC	Goat IgG $F(ab')_2$	-	Biosource	
	PE	Mouse IgG1	SA-DA4	Southern Biotech	
Igκ	PE	Mouse IgG1	G20-193	BD Pharmingen	
Igλ	PE	Mouse IgG1	1-155-2	BD Pharmingen	
Ki67	-	Mouse IgG1	MIB-1	DAKO	
MHC-I	PE	Mouse IgG2a	3F10	Ancell	
MHC-II	PE	Mouse IgG1	TDR31.3	Ancell	
Pax5 (BSAP)	-	Mouse IgG2a	A-11	Santa Cruz	
RAG2 [C-19]	-	Goat IgG	-	Santa Cruz	
TACI	PE	Mouse IgG1	165604	R&D Systems	
Tryptase	-	Mouse IgG1	AA1	DAKO	

b. Immunofluorescence

Antigen | [Epitope]	**Label**	**Isotype**	**Clone (if monoclonal)**	**Manufacturer**	**Note**
AID	-	Rat IgG2b	EK2 5G9	Cell Signaling	
[C-20]	-	Goat IgG	-	Santa Cruz	
APRIL [N16]	-	Goat IgG	-	Santa Cruz	
ED2	-	Rabbit IgG	-	Prosci	
BAFF (CD257)	PE	Mouse IgG1	1D6	eBioscience	
	Biotin	Mouse IgG1	1D6	eBioscience	
	-	Rabbit IgG	-	Upstate	
BAFF-R (CD268)	-	Mouse IgG1	11C1	Abcam	
BCMA [N-16]	-	Goat IgG	-	Santa Cruz	
Blimp-1	-	Mouse IgG1	3H2-E8	Novus Biologicals	
CD5	PE	Mouse IgG1	UCHT2	BD Biosciences	
CD10	PE	Mouse IgG1	ALB1	Immunotech	

CD19	PE	Mouse IgG1	4G7	BD Biosciences	These two clones both show that tonsillar IgD plasmablasts are $CD19^{+}$.
	Biotin	Mouse IgG1	H1B19	BD Biosciences	
CD27	PE	Mouse IgG1	M-T271	Ancell	
CD117	PE	Mouse IgG1	104D2	BD Biosciences	
	-	Rabbit IgG	-	DAKO	
CD123	PE	Mouse IgG2a	7G3	BD Biosciences	
CD138	PE	Mouse IgG1	Mi15	BD Biosciences	
FcεRIα	Biotin	Mouse IgG2b	AER-37	eBioscience	
Ig	-	Goat $F(ab')_2$	-	Cappel	
IgD	FITC	Goat IgG $F(ab')_2$	-	Southern Biotech	
	Biotin	Goat IgG $F(ab')_2$	-	Southern Biotech	
IgM	FITC	Goat IgG $F(ab')_2$	-	Biosource	
	PE	Mouse IgG1	SA-DA4	Southern Biotech	
	Biotin	Goat IgG $F(ab')_2$	-	Southern Biotech	
	-	Goat IgG $F(ab')_2$	-	Caltag	
Igκ	PE	Mouse IgG1	G20-193	BD Pharmingen	
	-	Goat IgG $F(ab')_2$		Caltag	
Igλ	PE	Mouse IgG1	1-155-2	BD Pharmingen	
	-	Goat IgG $F(ab')_2$		Caltag	
Ki67	-	Mouse IgG1	MIB-1	DAKO	
LL-37	-	Rabbit IgG	-	PANATecs GmbH	
Pax5 (BSAP)	-	Mouse IgG2a	A-11	Santa Cruz	
RAG2 [C-19]	-	Goat IgG	-	Santa Cruz	
TACI [C-20]	-	Goat IgG	-	Santa Cruz	
Tryptase	-	Mouse IgG1	AA1	DAKO	

Table S2 Primers used in regular and quantitative real-time PCR

Target Gene		Primer sequence	T_m Used (ºC)
ACTB	S	GGATGCAGAAGGAGATCACT	58
	AS	CGATCCACACGGAGTACTTG	
CAMP	S	GTCACCAGAGGATTGTGACTTCAA	58
	AS	TTGAGGGTCACTGTCCCCATA	
CRP	S	ATACACTGTGGGGGCAGAAG	58
	AS	CCGCCAAGATAGATGGTGTT	
DEFB103A	S	TATCTTCTGTTTGCTTTGCTCTTC	58
	AS	CCTCTGACTCTGCAATAATATTTCTGTAA	
PTX3	S	GGGACAAGCTCTTCATCATGCT	58
	AS	GTCGTCCGTGGCTTGCA	
SPAG11A/F	S	CTGTTTCCAGGATCGTCTCA	58
	AS	GAGATGTGCACTTGGTAAGG	
SPAG11D/G	S	CTGTTTCCAGGATCGTCTCA	58
	AS	GGAACATCCCCTTGGTAAGG	

Nature Immunology: doi:10.1038/ni.1748

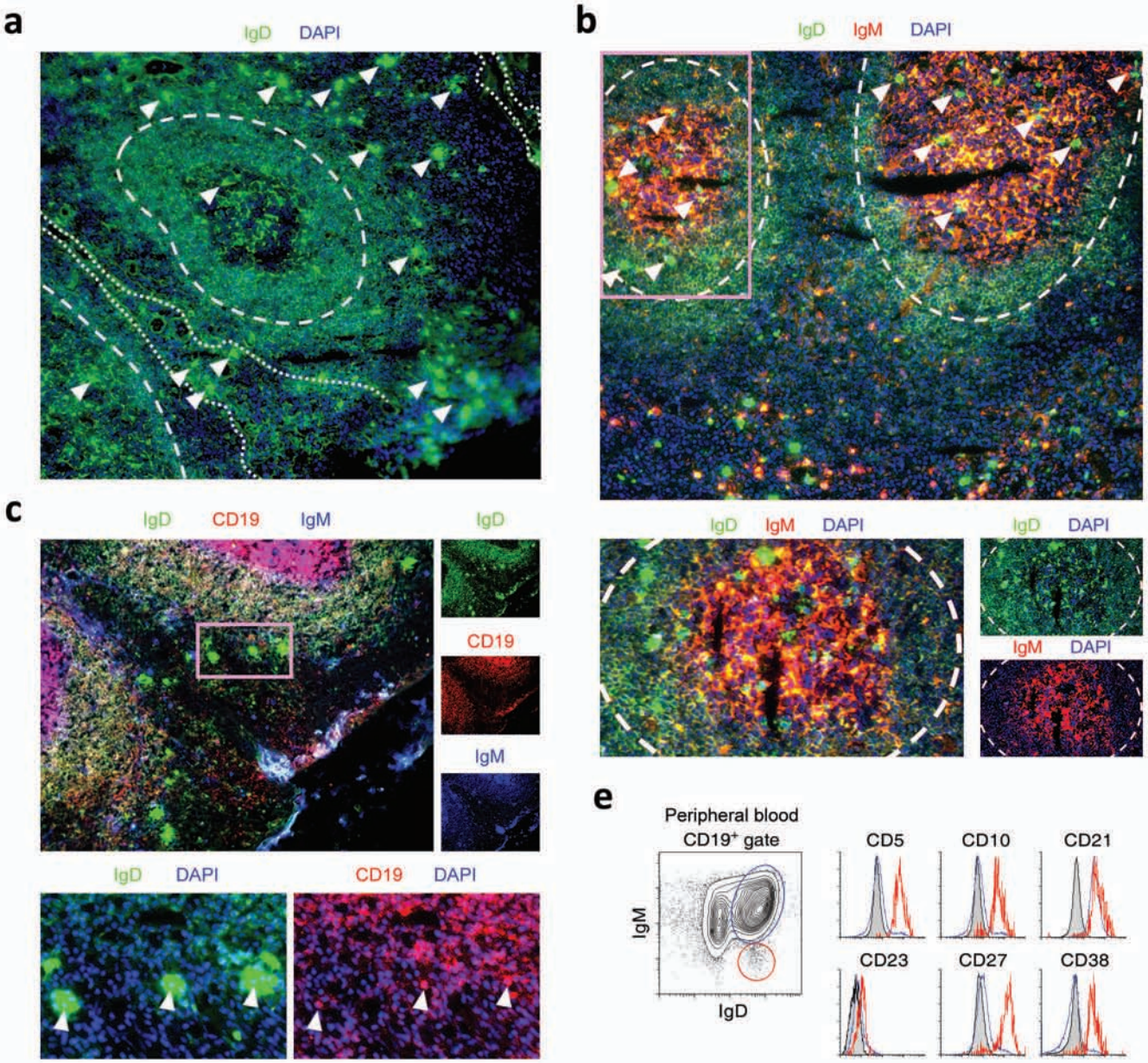

Nature Immunology: doi:10.1038/ni.1748

Chen *et al.*, Fig. S1

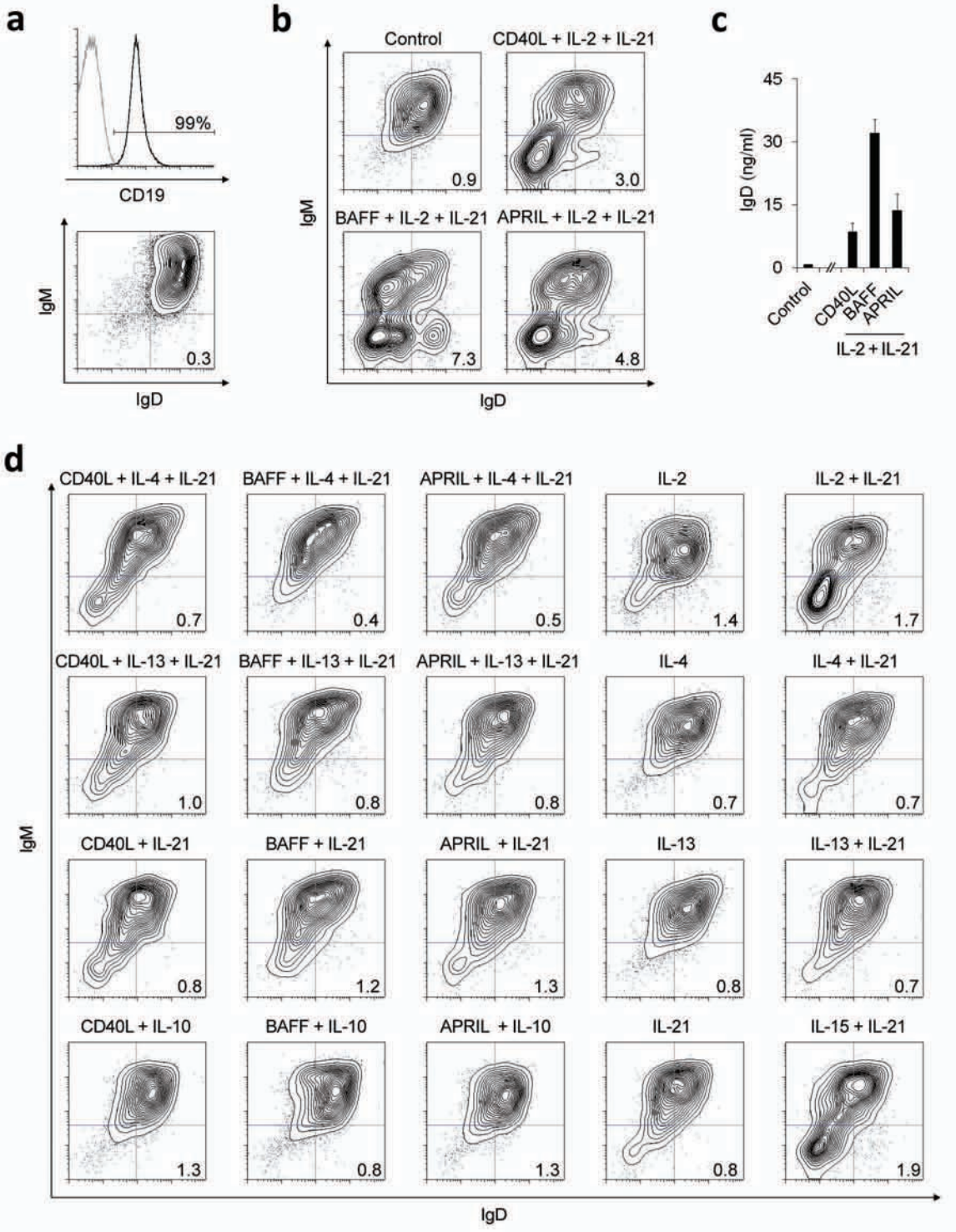

Nature Immunology: doi:10.1038/ni.1748

Chen *et al.*, Fig. S2

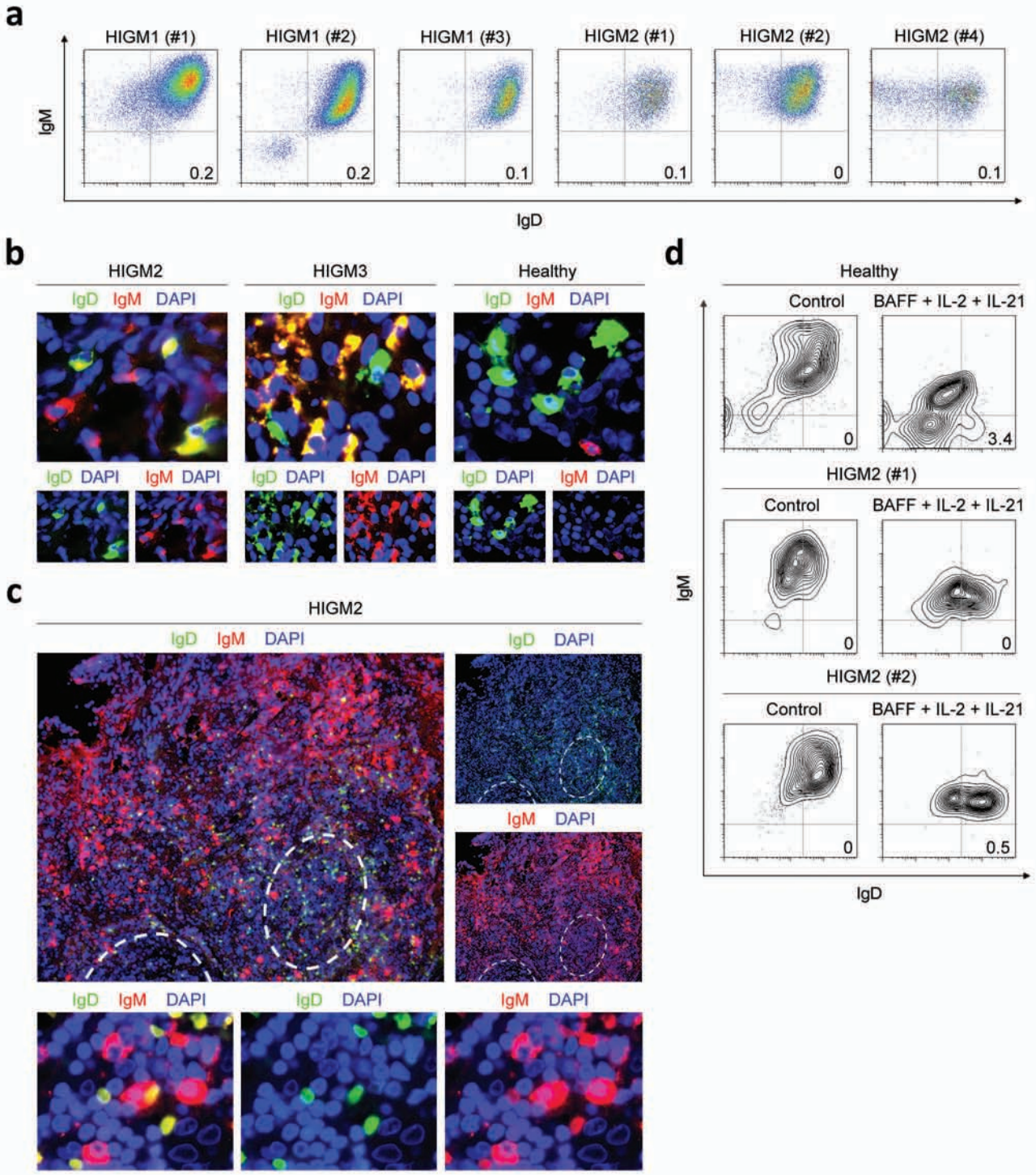

Nature Immunology: doi:10.1038/ni.1748

Chen *et al.*, Fig. S3

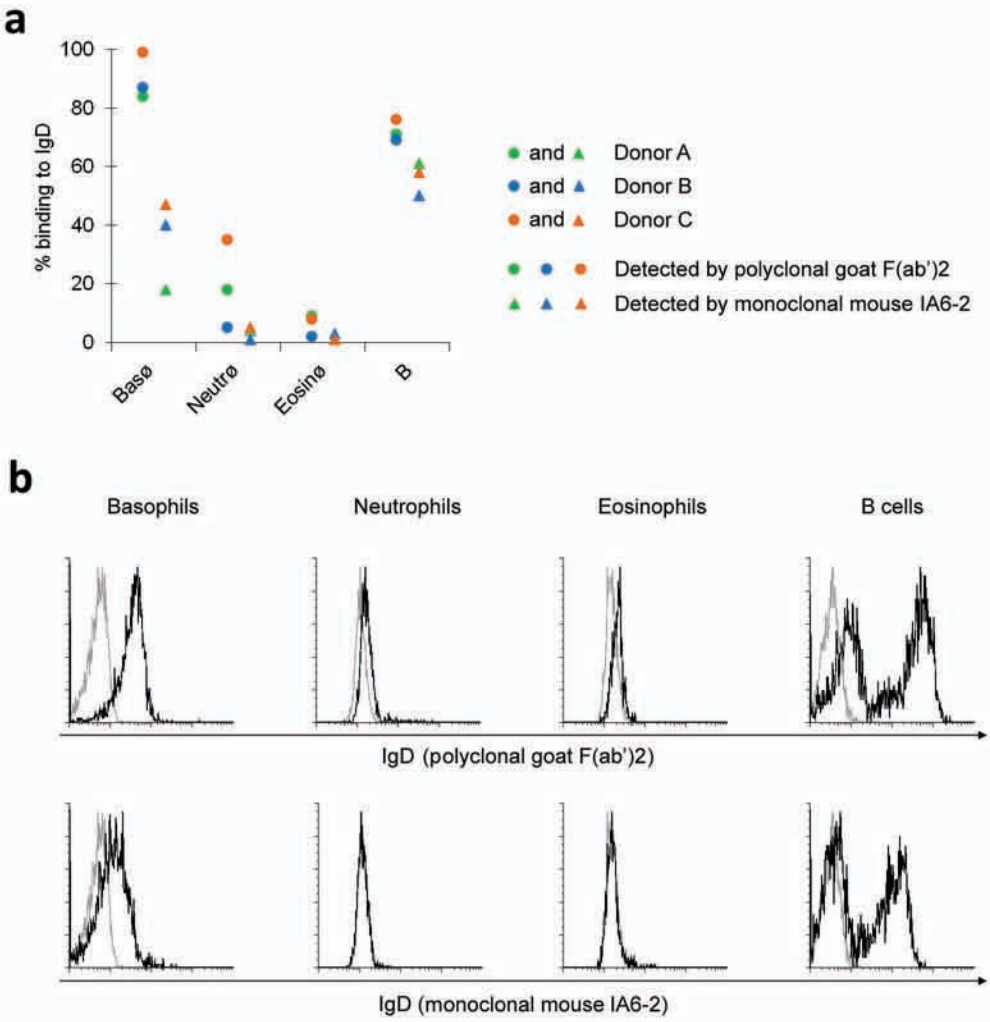

Nature Immunology: doi:10.1038/ni.1748

Chen *et al.*, Fig. S4

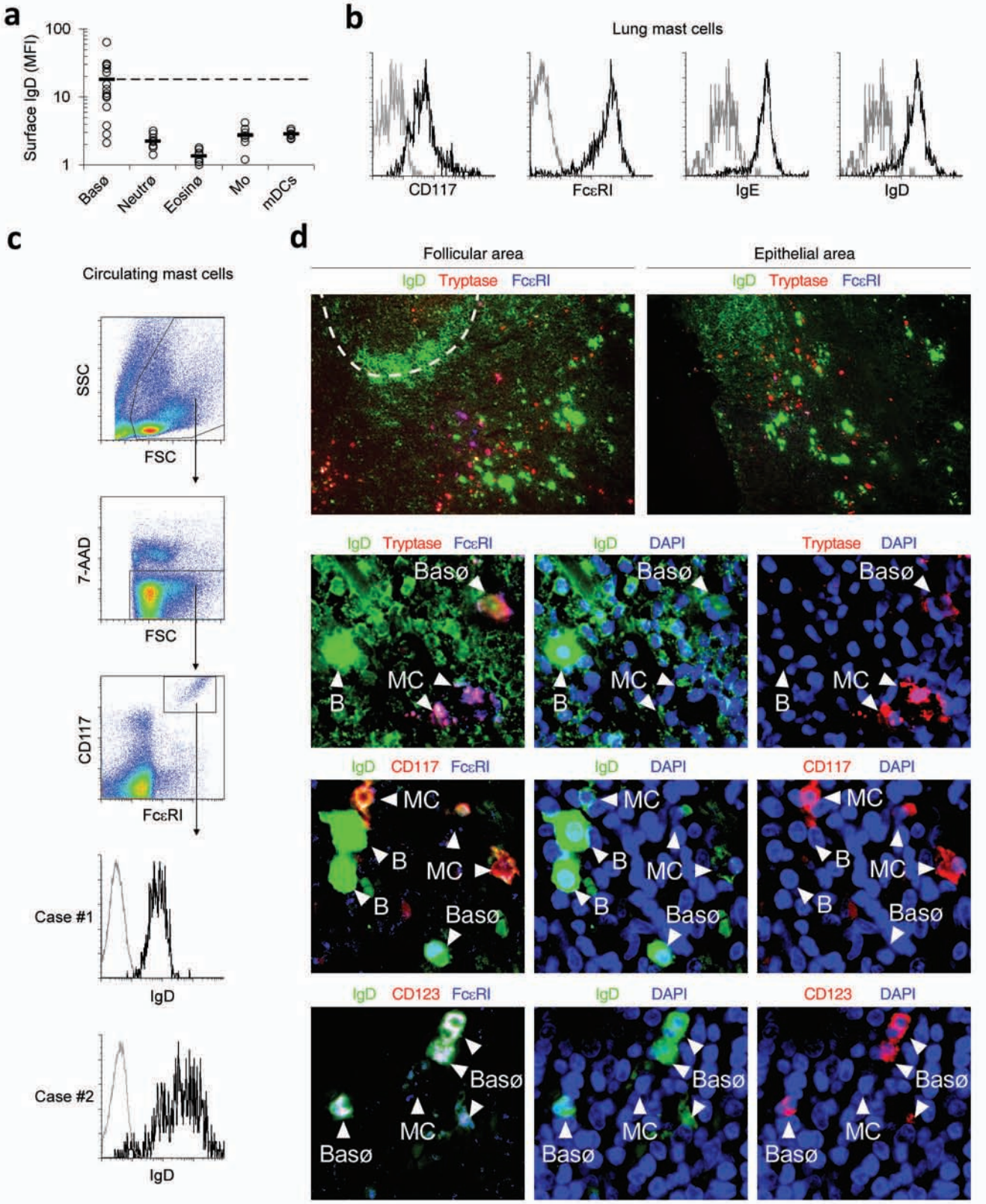

Nature Immunology: doi:10.1038/ni.1748

Chen *et al.*, Fig. S5

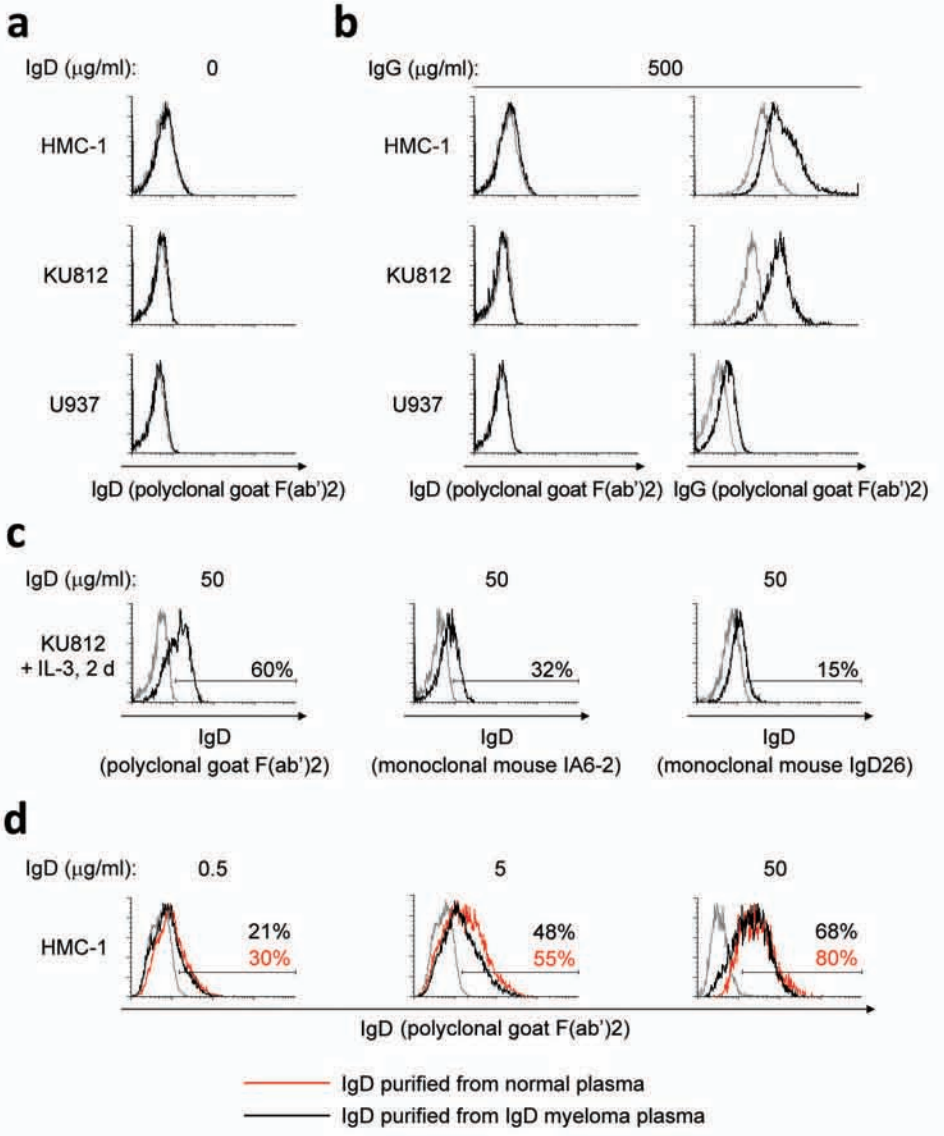

Nature Immunology: doi:10.1038/ni.1748

Chen *et al.*, Fig. S6

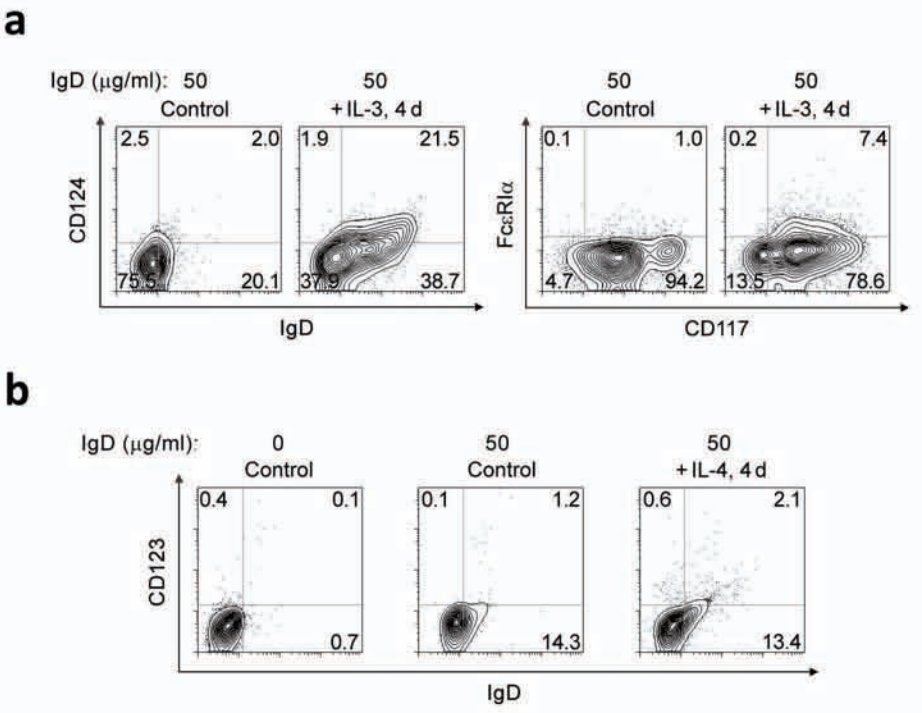

Nature Immunology: doi:10.1038/ni.1748

Chen *et al.*, Fig. S7

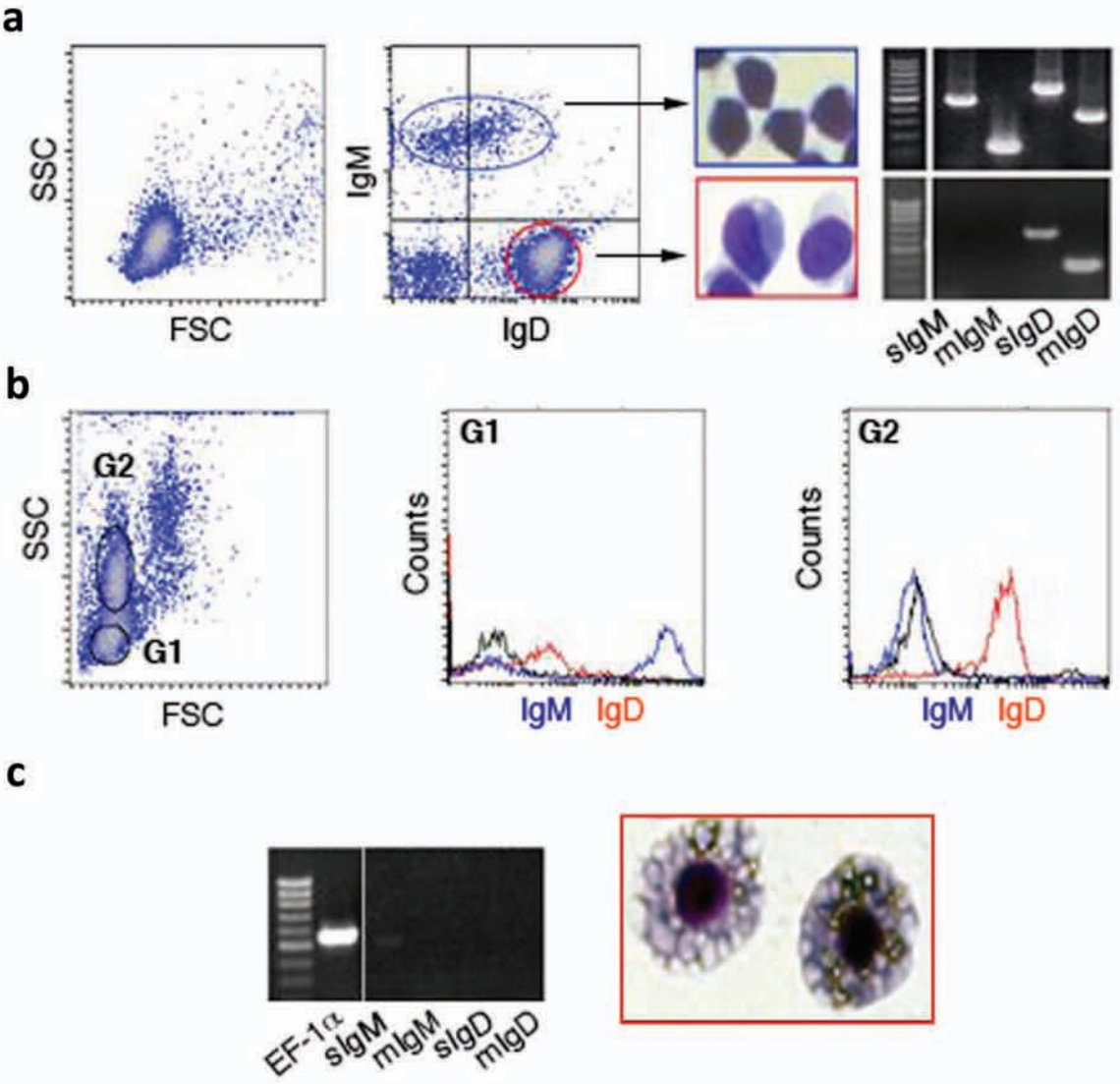

Nature Immunology: doi:10.1038/ni.1748

Chen *et al.*, Fig. S8

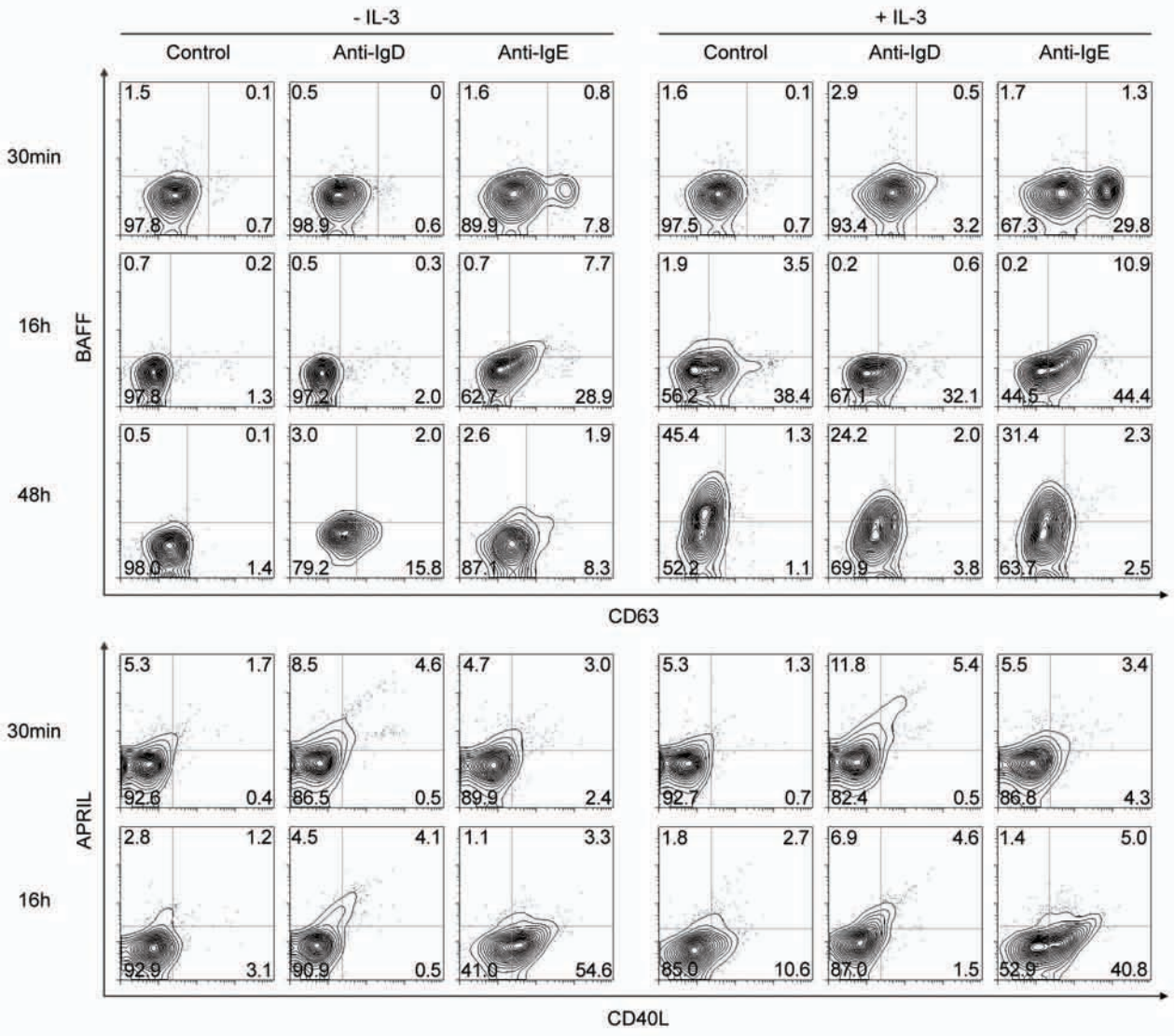

Nature Immunology: doi:10.1038/ni.1748

Chen *et al.*, Fig. S9

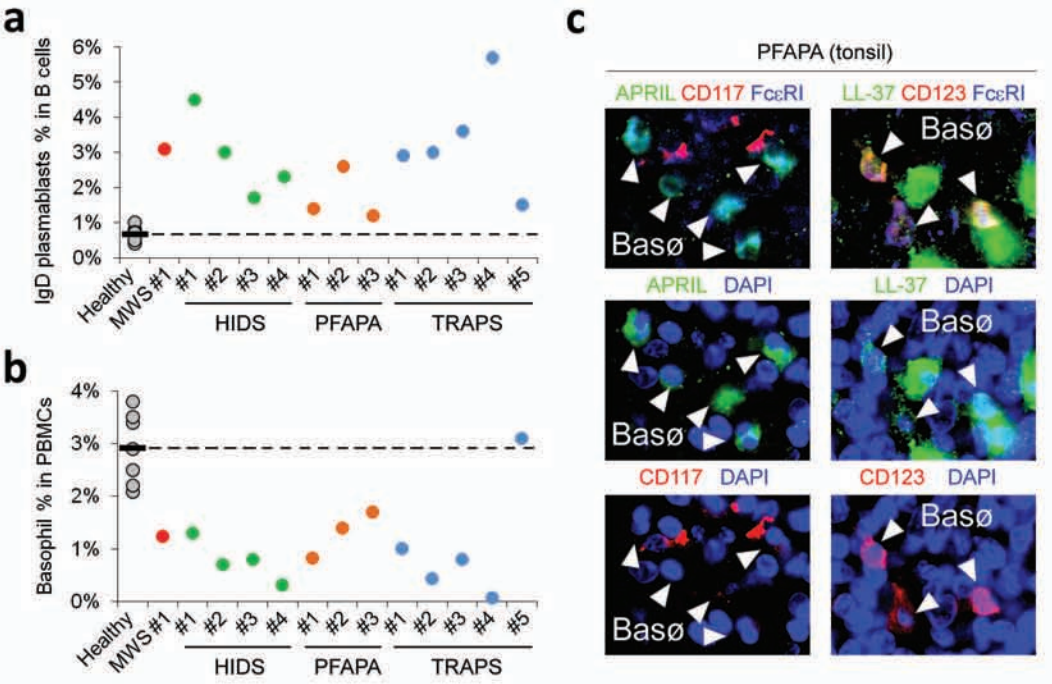

Nature Immunology: doi:10.1038/ni.1748

Chen *et al.*, Fig. S10

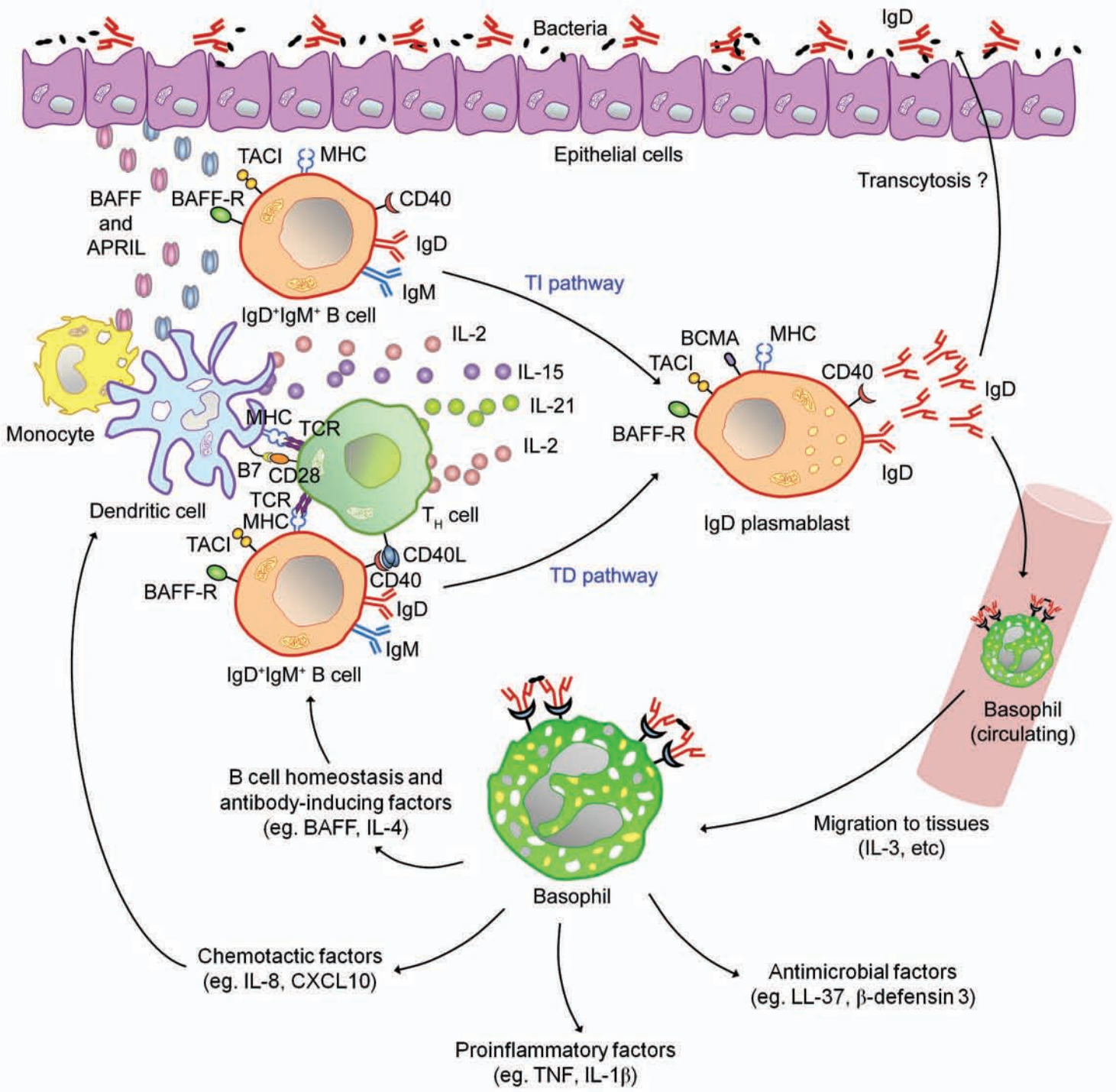

Nature Immunology: doi:10.1038/ni.1748

Chen *et al.*, Fig. S11